Subseafloor sedimentary life in the South Pacific Gyre

Steven D'Hondt[a,1], Arthur J. Spivack[a], Robert Pockalny[a], Timothy G. Ferdelman[b], Jan P. Fischer[b], Jens Kallmeyer[c], Lewis J. Abrams[d], David C. Smith[a], Dennis Graham[a], Franciszek Hasiuk[e], Heather Schrum[a], and Andrea M. Stancin[e]

[a]Graduate School of Oceanography, University of Rhode Island, Narragansett Bay Campus, South Ferry Road, Narragansett, RI 02882; [b]Max Planck Institute for Marine Microbiology, Celsiusstrasse 1, D-28359 Bremen, Germany; [c]Department of Geosciences, University of Potsdam, Haus 27, Zi. 0.34, Karl-Liebknecht-Strasse 24, 14476 Golm, Germany; and [d]Department of Geography and Geology, University of North Carolina at Wilmington, DeLoach Hall, 601 South College Road, Wilmington, NC 28403; and [e]Department of Geological Sciences, University of Michigan, 2534 C.C. Little Building, 1100 North University Avenue, Ann Arbor, MI 48109

Edited by Edward F. DeLong, Massachusetts Institute of Technology, Cambridge, MA, and approved May 6, 2009 (received for review November 23, 2008)

The low-productivity South Pacific Gyre (SPG) is Earth's largest oceanic province. Its sediment accumulates extraordinarily slowly (0.1–1 m per million years). This sediment contains a living community that is characterized by very low biomass and very low metabolic activity. At every depth in cored SPG sediment, mean cell abundances are 3 to 4 orders of magnitude lower than at the same depths in all previously explored subseafloor communities. The net rate of respiration by the subseafloor sedimentary community at each SPG site is 1 to 3 orders of magnitude lower than the rates at previously explored sites. Because of the low respiration rates and the thinness of the sediment, interstitial waters are oxic throughout the sediment column in most of this region. Consequently, the sedimentary community of the SPG is predominantly aerobic, unlike previously explored subseafloor communities. Generation of H_2 by radiolysis of water is a significant electron-donor source for this community. The per-cell respiration rates of this community are about 2 orders of magnitude higher (in oxidation/reduction equivalents) than in previously explored anaerobic subseafloor communities. Respiration rates and cell concentrations in subseafloor sediment throughout almost half of the world ocean may approach those in SPG sediment.

aerobic | biomass | oxic | radiolysis | respiration

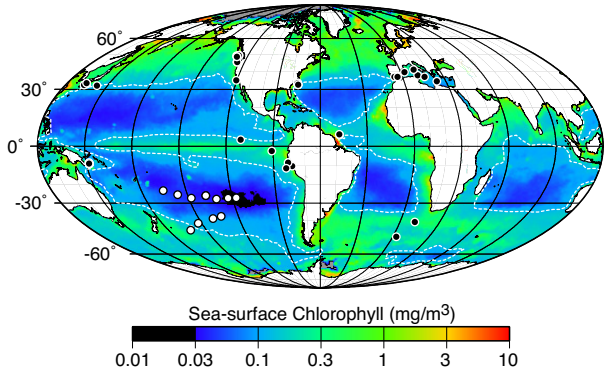

Fig. 1. Site locations on a map of time-averaged sea-surface chl-a concentrations [Global SeaWiFS Chlorophyll (mean of September 1997–December 2004)]. White dots mark sites analyzed for this study. Black dots mark sites previously analyzed for subseafloor biomass and/or activity (2, 3). Dashed white lines delimit the area in each gyre where the sea-surface chlorophyll-a (chl-a) concentration is ≤0.14 mg/m^3.

Life is previously unknown in the subseafloor sediment of the vast low-productivity regions that dominate the open ocean. Past studies have focused on sites relatively close to shore and beneath major upwelling zones (1–4) (Fig. 1), where biological productivity and organic flux to the seafloor are generally high (5). Their subseafloor [greater than 1.5 m below seafloor (mbsf)] sedimentary communities contain abundant living microbes (6–9). These communities (10, 11) and their metabolic activities (3, 12) are diverse. Their activities are dominated by fermentation, sulfate reduction, and methanogenesis (13). Their principal food source is buried organic matter from the surface world (3). The environmental properties of these previously sampled sites differ greatly from environmental properties throughout most of the open ocean, where oceanic productivity and organic flux to the seafloor are very low (5).

To understand the extent and nature of subseafloor life in the low-productivity heart of the ocean, expedition Knox-02RR surveyed and cored the sediment at 10 sites throughout the South Pacific Gyre (SPG) and at 1 site at its southern margin (Fig. 1). The central SPG has been described as Earth's largest oceanic desert (14). The middle of the gyre is farther from continents and productive oceanic regions than any other site on Earth. It contains the clearest seawater in the world (15). Its organic flux to the seafloor is extremely low (5). The area of its low-chlorophyll [≤0.14 mg of chlorophyll-a/m^3 (chl-a/m^3)] region (5.2×10^7 km^2) is more than twice the area of North America (equal to ≈19,000 Rhode Islands) (Fig. 1). Its subseafloor ecosystem has never before been explored.

Results

Sedimentation and Organic Burial. The cored sediment ranged in age from 0 to 70 Ma and in depth below seafloor from 0 to 9 m (Table 1). Total sediment thickness ranges from 1 m (SPG-7) to 130 m (SPG-12) (determined from 3.5-kHz sonar and seismic reflection profiles). At the deepest water sites in the low-chlorophyll region of the SPG (sites SPG-1 to SPG-4 and SPG-9 to SPG-11), the cored sediment is homogeneous brown clay capped by a nearly continuous layer of manganese (Mn) nodules. Discrete horizons of Mn nodules or Mn crust also occur deeper in the cored sediment at SPG-1 and SPG-10. Silt and sand-sized Mn nodules and cosmic debris commonly occur within the brown clay, but fossils, except for scattered ichthyoliths, do not. The cored sediment at the shallowest sites (SPG-6 and SPG-7) is calcareous nannofossil-bearing clay. The sediment at SPG-5 is transitional between these 2 lithologies. Site SPG-12 lies outside the low-chlorophyll region, and its cored sediment is dominantly siliceous ooze with abundant diatom debris and sponge spicules.

Mean sedimentation rates are extremely low in the low-chlorophyll region of the SPG (17) (Table 1). In general, they are lowest at sites where the seafloor is below the calcite compensation depth [≈4,500 m below sea level in this region (18)] and sea-surface chlorophyll concentrations are below 0.1 mg chl/m^3. Mean sedimentation rate is higher at our eastern-most sites, where water depth is shallowest (allowing carbonate sediment to accumulate), and at our western-most sites, where sea-surface chlorophyll content is above 0.1 mg chl/m^3 and the sites were south of the central gyre many tens of millions of years ago. The rate

Author contributions: S.D., A.J.S., R.P., and T.G.F. designed research; S.D., A.J.S., R.P., T.G.F., J.P.F., J.K., L.J.A., D.C.S., D.G., F.H., H.S., and A.M.S. performed research; S.D., A.J.S., R.P., T.G.F., J.P.F., J.K., L.J.A., D.C.S., D.G., F.H., H.S., and A.M.S. analyzed data; and S.D. wrote the paper.

The authors declare no conflict of interest.

This article is a PNAS Direct Submission.

Freely available online through the PNAS open access option.

[1]To whom correspondence should be addressed. E-mail: dhondt@gso.uri.edu.

ENVIRONMENTAL SCIENCES

Table. 1. Sediment properties and subseafloor (>1.5 mbsf) biogeochemical fluxes

Site	latitude	longitude	Basement age (16) (Ma)	water depth (m)	Total sediment thickness (m)	Cored sediment (mbsf)	Sedimentation rate (cm/kyr)	Organic carbon content at 0–5 cmbsf (dry weight %)	Organic carbon burial rate at ≈0–5 cmbsf (molC/cm²/yr)	Organic carbon burial rate at ≈150 cmbsf (molC/cm²/yr)	Downward O_2 flux at 1.5 mbsf (mol/cm²/yr)	Upward NO_3^- flux at 1.5 mbsf (mol/cm²/yr)	Radiolytic H_2 production (mol H_2/cm²/yr)
SPG-1	−23°51′	−165°39′	100	5697	71	7.79	0.031	0.33	3.6E−09	1.6E−09	−2.0E−08	6.9E−10	1.4E−08
SPG-2	−26°03′	−156°54′	100	5127	17	8.20	0.017	0.53	3.2E−09	8.7E−10	−6.8E−09	3.5E−10	3.1E−09
SPG-3	−27°57′	−148°35′	71	4852	5.49	5.49	0.008	0.42	1.2E−09	4.4E−10	−4.1E−09	5.4E−10	8.0E−10
SPG-4	−26°29′	−137°56′	33.5	4285	9	7.24	0.028	0.42	4.2E−09	1.6E−09	−5.4E−09	n.d.	1.6E−09
SPG-5	−28°27′	−131°23′	24.1	4221	17	8.05	0.069	0.36	8.8E−09	3.8E−09	−7.6E−09	n.d.	3.0E−09
SPG-6	−27°55′	−123°10′	13.5	3738	15	2.59	0.111	n.d.	n.d.	7.0E−09	−2.2E−08	n.d.	2.7E−09
SPG-7	−27°44′	−117°37′	6.1	3688	1.05	1.05	0.017	0.29	1.7E−09	n/a	n/a	n/a	n/a
SPG-9	−38°04′	−133°06′	39	4925	20	7.05	0.051	0.38	9.5E−09	3.8E−09	−2.8E−09	3.0E−10	4.5E−09
SPG-10	−39°19′	−139°48′	58	5283	21	5.63	0.037	0.56	1.0E−08	2.0E−09	−1.2E−08	6.0E−10	4.8E−09
SPG-11	−41°51′	−153°06′	75	5076	67	2.98	0.089	0.51	2.2E−08	8.2E−09	−2.4E−09	1.6E−09	1.6E−08
SPG 12	−45°58′	−163°11′	73	5306	130	4.98	0.178	0.34	3.0E−08	2.7E−08	n/a	−3.1E−08	n.d

n/a, not applicable; n.d., not determined.

Fig. 2. Cell concentrations in subseafloor sediment. White dots mark data from SPG sites SPG-1 to SPG-11, and white triangles mark data from site SPG-12, just outside the gyre (this study). Black dots mark data from all other sites (2, 3).

is highest at SPG-12, just outside the central gyre, because of sedimentation of siliceous debris. Mean sedimentation rates within the SPG are among the lowest that occur at the Earth's surface. The highest SPG rates are, respectively, 1 and 2 orders of magnitude lower than rates at equatorial Pacific and Peru Margin sites, where subseafloor life has previously been studied (19, 20).

Organic carbon burial rates at the sediment surface in the brown clay-dominated sites of the low-chlorophyll region are also extremely low (Table 1). The highest of these is more than 1 order of magnitude lower than organic carbon burial rates at sites where subseafloor sedimentary life has previously been studied [e.g., 4.5×10^{-7} mol C/cm^2 annually at equatorial Pacific Ocean Drilling Program (ODP) Sites 1225 and 1226 and 3.1×10^{-6} mol C/cm^2 annually at Peru Margin ODP Sites 1227 and 1230 (3)].

Most of the buried organic matter is oxidized in the shallowest portion of the sediment column. Burial of total organic carbon (TOC) below 1.5 mbsf ranges from 4.4×10^{-10} to 8.2×10^{-9} mol C/cm^2 annually (Table 1). TOC declines very little with increasing depth below the initial few tens of centimeters below seafloor (cmbsf); for example, at SPG-3, it declines from 0.52% at 3 cmbsf to 0.26% at 23 cmbsf and 0.17% at 1.47 mbsf but then declines more slowly to 0.09% at the base of the sediment column (5.17 mbsf). If the TOC burial rate has been relatively constant over the 70 million years of sedimentation at SPG-3, the relative constancy of TOC content at depths greater than a few centimeters below seafloor indicates that organic matter at those depths is so recalcitrant or inaccessible that almost none of it has been oxidized since passing through the near-surface zone in its initial few million years after burial.

Microbial Biomass. Despite the extraordinarily low rate of organic burial, microbes occur throughout the cored sediment columns (Fig. 2), indicating that biomass persists in the sediment for at least 70 million years (compare Fig. 2 and Table 1). However, cell abundance is extremely low; the average counted concentration at each depth below the seafloor at SPG sites 1–11 is 3 to 4 orders of magnitude lower than the average of all previously explored subseafloor sediment populations at the same depths (Fig. 2). Throughout much of the sediment column at these sites, cell concentrations are below the detection limit of standard counts in slurried sediment. Consequently, our counts are based on populations of cells separated from the sediment (21). Although

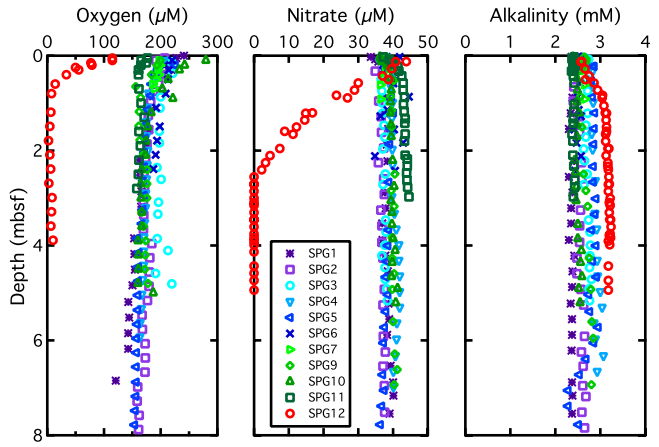

Fig. 3. Dissolved chemical concentrations in subseafloor sediment of the SPG sites: O_2 (*Left*), NO_3^- (*Center*), and alkalinity (*Right*).

counts of separated cells may slightly underestimate total cell concentrations, there are not significant differences between the results of the 2 techniques at SPG-12, where cell counts are typically above the detection limit of the standard technique. If the counts of separated cells underestimate total cell concentration by 10–30% (21), the effect is not significant on the orders-of-magnitude scale that distinguishes the SPG counts from counts of subseafloor populations in other regions (Fig. 2).

Chemical Evidence of Microbial Activity. Porewater chemistry indicates that O_2 is reduced and organic matter is oxidized within the sediment at all the cored sites. At the sites within the low-chlorophyll portion of the SPG, dissolved O_2 is the principal electron acceptor. It is present throughout the cored sediment columns. Its concentration decreases by tens of micromoles per liter within the initial few tens of centimeters below seafloor and then declines much more slowly with greater depth (Fig. 3 *Left*).

In contrast to O_2, NO_3^- increases slightly (by a few micromoles per liter at SPG-1 to SPG-4 and at SPG-10 to SPG-11) or exhibits no clear change (at SPG-5 to SPG-9) with depth (Fig. 3 *Center*); the slight increase is attributable to oxidation of buried organic nitrogen. Comparison with sparse data from Deep Sea Drilling Project (DSDP) Leg 92 sites (22) in the northern SPG at 20°S suggests that NO_3^- concentrations are probably at or above deep-water concentrations throughout the entire sediment column of the SPG. Just outside the low-chlorophyll region of the SPG, at SPG-12, O_2 disappears within 1 mbsf and NO_3^- disappears by 2.5 mbsf.

Dissolved SO_4^{2-} concentration is constant with depth below seafloor at all 11 sites. This result is not surprising for sites SPG-1 to SPG-11, because SO_4^{2-} is not reduced where dissolved O_2 and NO_3^- are available. Given the absence of dissolved O_2 below 1 mbsf and NO_3^- below 2.5 mbsf at SPG-12, the constancy of SO_4^{2-} with depth indicates that oxidized metals, such as iron and Mn, are the principal electron acceptors at greater depth in the sediment at SPG-12.

Alkalinity increases very slightly with depth at 5 sites in the low-chlorophyll region (SPG-2, SPG-4, SPG-7, SPG-9, and SPG-10) and exhibits no clear trend with depth at the remaining 5 sites in this region (SPG-1, SPG-3, SPG-5, SPG-6, and SPG-11). Alkalinity increases much more strongly with depth at SPG-12 than at any of the sites in the low-chlorophyll region. Alkalinity can be increased by oxic respiration because the carbon dioxide produced will dissolve carbonate if it is present. Nitrate reduction also produces alkalinity.

We calculated fluxes of O_2 downward into the subseafloor ecosystem and NO_3^- upward at all the sites within the central gyre where the dissolved chemical profiles are stable enough that fluxes can be calculated (Table 1). For these calculations, we followed the convention of previous studies by defining the subseafloor ecosystem as beginning at 1.5 mbsf (3, 13). At steady state, these fluxes are nearly equal to the net rate of O_2 reduction and the net rate of NO_3^- production by the entire subseafloor sedimentary ecosystem below 1.5 mbsf at each site (these fluxes are not exactly equal to the net subseafloor sedimentary reaction rates because they do not account for fluxes across the sediment/basement interface). The upward NO_3^- flux cannot be calculated (*i*) at SPG-4 and SPG-6 because no clear trend occurs in their dissolved NO_3^- concentration profiles or (*ii*) at SPG-5 because its dissolved NO_3^- concentration decreases with depth.

These O_2 fluxes demonstrate that an active microbial community is present in the subseafloor at these sites, despite the very low concentrations of chlorophyll in the overlying ocean and the extraordinarily low rate of organic matter input. The NO_3^- production rates at SPG-1 to SPG-3 and SPG-9 to SPG-11 indicate that this activity is partly fueled by oxidation of nitrogen from buried organic matter.

Just outside the central gyre at SPG-12, dissolved O_2 disappears well above 1.5 mbsf and the subseafloor ecosystem is characterized by net reduction of NO_3^- rather than net production. The downward flux of NO_3^- past 1.5 mbsf is 2.6×10^{-8} mol/cm^2 annually. Because NO_3^- disappears before 2.5 mbsf at SPG-12, this flux fuels respiration for only the shallowest fraction of the subseafloor community at this site.

Radiolytic H_2 Production. H_2 is naturally produced by radiolysis of water in any environment where water is bombarded by α-, β-, and γ-radiation produced during radioactive decay. Radiolytic H_2 has been identified as a significant electron donor in deep continental aquifers where organic products of photosynthesis are largely absent (23). It may also be a significant electron donor in marine sediment where organic matter is scarce. Radiolytic H_2 production is particularly efficient in deep-sea clays because all the α particles produced in the clay escape from the clay grains and travel through water before being stopped (24). We estimate that the radiolytic production of dissolved H_2 at these sites is 1×10^{-12} mol/cm^3 sediment per year (at SPG-1 to SPG-6) to 1.2×10^{-12} mol/cm^3 sediment per year (at SPG-9 to SPG-11). Total H_2 production by this process varies from site to site with thickness of the sediment column; it ranges from 1.6×10^{-8} mol H_2/cm^2 annually at SPG-11 to 8.0×10^{-10} mol H_2/cm^2 annually at SPG-3 (Table 1).

To assess potential microbial use of radiolytic H_2, we calculated the H_2 concentrations that would be expected if H_2 were not consumed in the sediment column. For these calculations, we considered 2 cases: first, assuming there is a sink for H_2 in the underlying basalt and, second, assuming the basalt is impermeable to H_2. These 2 cases bracket the range of possibilities for the bottom boundary condition. H_2 production, diffusivity, porosity, and tortuosity were assumed to be constant with depth. If radiolytic H_2 is not consumed, its peak concentration scales with the square of the thickness of the sediment column. Sites SPG-1 and SPG-3 provide examples of the predicted H_2 concentrations. For SPG-1, predicted peak concentration at the base of the cored section (7.81 mbsf) is between 25 and 26 μM. For SPG-3, 5.5 m in length, predicted peak concentration is between 0.32 and 0.64 μM.

Measured H_2 concentrations are consistently far below these calculated values. No H_2 was detected in any of the 154 samples from sites SPG-1 through SPG-11, except for a single sample at SPG-10 (the detection limit ranged from 2–229 nM). The scarcity of H_2 at all sites indicates that radiolytic H_2 is removed as quickly as it is generated, as expected from in situ microbial utilization.

Discussion

An Aerobic Subseafloor Ecosystem. In electron (oxidation/reduction) equivalents, O_2 fluxes down past 1.5 mbsf in the SPG are nearly equal to the rates at which organic carbon is buried below 1.5 mbsf (Table 2). However, the O_2 flux slightly exceeds this organic carbon

Table 2. Rates of subseafloor activities and biogeochemical fluxes (in electron equivalents) per unit area and per cell

Site	Subseafloor O_2 reduction rate (mol e-/cm²/yr)	Subseafloor NO_3^- reduction rate (mol e-/cm²/yr)	O_2 reduction rate based on net NO_3^- production (mol e-/cell/yr)	Organic carbon burial rate at 1.5 mbsf (mol e-/cm²/yr)	Radiolytic H_2 production rate (mol e-/cm²/yr)	Total cells below 1.5 mbsf	O_2 reduction rate per cell (mol e-/cell/yr)	O_2 reduction rate per cell based on net NO_3^- production (mol e-/cell/yr)	Organic carbon burial rate per cell (mol e-/cell/yr)	Radiolytic H_2 production rate per cell (mol e-/cell/yr)
SPG-1	7.9E−08	n/a	7.1E−09	8.2E−09	2.7E−08	8.9E+07	8.9E−16	8.0E−17	9.3E−17	3.1E−16
SPG-2	2.7E−08	n/a	3.6E−09	4.3E−09	6.2E−09	2.6E+06	1.0E−14	1.4E−15	1.7E−15	2.4E−15
SPG-3	1.6E−08	n/a	5.6E−09	2.2E−09	1.6E−09	1.7E+06	9.6E−15	3.2E−15	1.3E−15	9.3E−16
SPG-4	2.2E−08	n/a	n.d.	7.8E−09	3.2E−09	4.7E+06	4.7E−15	n.d.	1.7E−15	6.9E−16
SPG-5	3.0E−08	n/a	n.d.	1.9E−08	6.0E−09	n.d.	n.d.	n.d.	n.d.	n.d.
SPG-6	8.9E−08	n/a	n.d.	3.5E−08	5.4E−09	n.d.	n.d.	n.d.	n.d.	n.d.
SPG-7	n/a	n/a	n/a	n/a	n/a	n/a	n/a	n/a	n/a	n/a
SPG-9	1.1E−08	n/a	3.0E−09	1.9E−08	8.9E−09	1.5E+06	7.6E−15	2.1E−15	1.3E−14	6.1E−15
SPG-10	4.8E−08	n/a	6.1E−09	1.0E−08	9.7E−09	1.0E+06	4.6E−14	5.9E−15	9.7E−15	9.3E−15
SPG-11	9.4E−09	n/a	1.6E−08	4.1E−08	3.2E−08	7.8E+06	1.2E−15	2.1E−15	5.3E−15	4.1E−15
SPG-12	n/a	−1.3E−07	n.d.	1.3E−07	n.d.	n.d	n.d.	n.d.	n.d.	n.d.

n/a, not applicable; n.d., not determined.

burial rate (by a factor of 2–10) at all but 2 of the sites (Table 2). This difference is exacerbated by the evidence from SPG-3 that most of the organic matter below 1.5 mbsf does not get oxidized, even on time scales of many tens of millions of years.

The difference between the O_2 flux and the TOC burial rate at these sites has several possible explanations: (*i*) a significant fraction of the O_2 may be diffusing through the sediment to the underlying basalt, (*ii*) the burial rate of organic carbon may have been slightly higher in the very distant past (tens of millions of years ago) than in the past several million years, or (*iii*) some of the O_2 flux oxidizes inorganic chemicals (e.g., reduced iron) in the sediment.

The initial explanation likely applies at most, perhaps all, of the sites from SPG-1 to SPG-11, because dissolved O_2 concentrations decline very slightly with sediment depth and extrapolations of the concentration profiles predict O_2 to be present throughout the entire sediment column at most or all of the sites (25). This explanation is also consistent with estimates of O_2 reduction derived from rates of subseafloor NO_3^- production (Table 2). These estimates assume that the carbon/nitrogen (C/N) ratio of buried organic matter approximates the Redfield ratio: 106:16. Estimated in this manner, the average organic-fueled O_2 reduction rate in the subseafloor sediment of our SPG sites is only about 20% of the average downward O_2 flux at the SPG sites and less than half of the average rate of TOC burial below 1.5 mbsf.

The inference that porewater is oxic throughout the sediment column in most of the SPG has 2 major implications. First, this subseafloor sedimentary community is predominantly aerobic, unlike previously explored deep subseafloor communities. Second, the flux of O_2 through the sediment may sustain aerobic life in the underlying basalt, which ranges in age to more than 100 Ma.

These relatively short geochemical profiles do not allow us to quantify precisely how much of the O_2 flux is going to sustain microbial respiration in the sediment and how much is going to oxidize the underlying basalt. Precise separation of these 2 rates requires drilling of the entire sediment column at several sites to determine the rate at which dissolved O_2 migrates from the sediment to the basalt.

Relation to Oceanographic Properties. Even if most of the O_2 flux is used to sustain respiration within the sediment at most of the SPG sites, subseafloor sedimentary rates of net respiration are much lower in this region than at all previously explored sites. In electron equivalents, the average O_2 flux into the subseafloor ecosystem at the SPG sites (3.7×10^{-8} mol e-/cm^2 annually) corresponds to a net respiration rate that is a factor of 5.4 lower than the rate of organic-fueled subseafloor respiration in the lowest activity site previously explored (Peru Basin ODP Site 1231 on the eastern edge of the SPG) and a factor of 550 less than the rate at the highest respiration site previously explored (Peru Margin ODP Site 1230) [Site 1230 and 1231 rates were taken from the work of D'Hondt et al. (3)]. These differences between sites are even greater when O_2 reduction is estimated from the rate of subseafloor NO_3^- production (Table 2); calculated in this manner, the mean organic-fueled O_2 reduction in the subseafloor sediment of our SPG sites (7×10^{-9} mol e-/cm^2 annually) is a factor of 28 lower than the rate of organic-fueled respiration at ODP Site 1231 and a factor of 2,910 lower than the rate of organic-fueled respiration at Site 1230. Subseafloor cell abundance is also much lower (by 3 to 4 orders of magnitude on average) in the central SPG than at all previously studied sites (Fig. 2).

These very low cell concentrations and net respiration rates mirror basic oceanographic properties of the SPG. Sea-surface chlorophyll concentrations, organic carbon burial rate, and sediment accumulation rate are all extremely low throughout the region. Sea-surface chlorophyll and productivity are low because the region is far from coastal and other regions of strong upwelling. Organic carbon burial rate is low because sea-surface chlorophyll, biological productivity, and sediment accumulation rates are low.

Sedimentation rate is low because (*i*) the low productivity results in a very low production rate of biogenic debris; (*ii*) the great distance from shore leads to very low sediment transport from land; and (*iii*) throughout much of the region, the seafloor is below the carbonate compensation depth, and biogenic carbonate consequently dissolves in the water column and at the seafloor.

Potential Reliance on Radiolytic H_2 Production. Our calculations indicate that generation of H_2 by radiolysis of the interstitial water is a significant electron donor source for this community. In electron equivalents, we estimate the rate of H_2 production by water radiolysis at sites SPG-1, SPG-2, SPG-3, SPG-10, and SPG-11 to approach or exceed the rate of organic carbon burial below 1.5 mbsf (Table 2). This equivalence implies that radiolysis of water provides roughly half of the electron donors used by the subseafloor sedimentary community at these sites and buried organic matter provides the other half, if all the organic matter is completely used. If less of the organic matter is used, as indicated by the constancy of TOC concentration with depth at SPG-3, radiolytic H_2 is the principal electron donor. Although microbial oxidation of this H_2 increases gross respiration in this ecosystem, it does not contribute to the net respiration calculated from downward O_2 fluxes because the release of O_2 by water radiolysis nearly stoichiometrically balances the O_2 used to oxidize the H_2 ($H_2O - > 1/2\ O_2 + H_2$).

H_2 from water radiolysis may be the principal electron donor in this sediment at depths greater than a few meters to a few tens of meters. Buried organic matter is probably the dominant food in the shallowest sediment because it tends to be oxidized at highest rates in shallow sediment and at successively lower rates in deeper (and older) sediment, where only the most recalcitrant or biologically inaccessible organic matter remains. In contrast, radiolytic H_2 production will be nearly constant throughout the sediment column if porosity, grain size, and concentrations of radioactive elements remain constant as our estimates assume; consequently, as organic oxidation declines with increasing depth below the seafloor in SPG sediment, H_2 from water radiolysis is likely to become the dominant food source. Recovery of the entire sediment column will ultimately be required to (*i*) quantify the respective roles of buried organic matter and radiolytic H_2 at each depth in the sediment column at each site and (*ii*) test if H_2 from water radiolysis is the dominant electron donor at depth in SPG sediment.

Respiration per Cell. Organic-fueled respiration per cell can be independently estimated from O_2 fluxes, NO_3^- fluxes, and organic carbon burial rates at 1.5 mbsf (Table 2). The first approach assumes that all the downward O_2 flux is used for oxidation of organic matter in the sediment. The second approach assumes that a Redfield C/N ratio (106:16) can be used to calculate the rate of organic oxidation from the rate of NO_3^- production (NO_3^- flux upward). The third approach assumes that the organic carbon burial rate has been constant over time. These approaches are subject to different uncertainties. The O_2-based rates are overestimates to the extent that O_2 migrates through the sediment to the underlying basalt. Uncertainties in estimates from NO_3^- fluxes may result from (*i*) NO_3^- produced in the sediment diffusing to the underlying basement (as well as to the overlying ocean) and (*ii*) C/N ratios of buried organic matter differing from the Redfield ratio if organic nitrogen is oxidized faster than organic carbon. Estimates from organic burial rates may be overestimates because they assume that all organic matter is eventually oxidized.

Potential gross respiration per cell can be estimated by adding any of the above estimates to the in situ rate of radiolytic H_2 production per cell (Table 2). With any of these approaches (O_2 flux, NO_3^- flux, or organic burial rate), gross respiration per cell is above rates necessary to counter aspartic acid racemization and DNA depurination (26).

Respiration per cell appears to be much higher in the oxic SPG sediment than in previously explored anoxic sediment; in electron equivalents, respiration per cell in the anoxic sediment of ODP Leg 201 ranges between 1×10^{-17} and 5×10^{-17} mol e-/cell annually [calculated from fluxes and cell counts of ODP Sites 1226, 1227, 1230, and 1231 (3, 27)]. This result is consistent with the calculation that the energy requirement for biomass synthesis by aerobes is more than 10 times the requirement for biomass synthesis by anaerobes (28).

Global Implications. These results have direct implications for global patterns of biomass and activity in subseafloor sediment. Several oceanographic properties are at their extreme in the center of the SPG (e.g., sea-surface chlorophyll concentration, distance from continents). The subseafloor sedimentary community of the central SPG is likely to define the low-biomass low-activity end-member for global distributions of subseafloor biomass and respiration. However, the other major ocean gyres resemble the SPG more closely than they resemble the regions where subseafloor life was previously explored. For example, sea-surface chlorophyll concentrations are below 0.14 mg chl/m^3 in all the major ocean gyres (Fig. 1). Consequently, rates of organic-fueled respiration, cell concentrations, and metabolic reliance on radiolytic H_2 in subseafloor sediment throughout almost half (48%) of the world ocean may approach the end-member values in SPG sediment.

Materials and Methods

TOC Content, Sedimentation Rate, and Burial Rates. TOC was measured at the University of Rhode Island using the technique of Verardo et al. (29) and a Costech ECS 4010 elemental analyzer. For sites SPG-2 to SPG-12, mean sedimentation rates were calculated from crust age and sediment thickness. For SPG-1, mean sedimentation rate was calculated from the 20.1 mbsf depth of the 65-Ma Cretaceous/Paleogene iridium anomaly at DSDP Site 596 (30). Organic carbon burial rates were calculated from TOC content and mean sedimentation rate and adjusted for porosity and wet bulk density. Surface burial of organic carbon is based on TOC content of 0–5 cmbsf at sites SPG-1 to SPG-11 and 10–15 cmbsf at site SPG-12. Burial of organic carbon at 150 cmbsf is based on TOC content of samples taken close to 150 cmbsf (between 143 and 167 cmbsf).

Sediment Physical Properties. Wet bulk density, grain density, and porosity were measured on discrete samples using the approach of Blum (31). Vertical conductivity measurements were performed shipboard with a Brinkmann/Metrohm Conductometer every 5 cm on cores throughout the cored sediment columns. The conductivity probe consisted of two 2-mm-diameter platinum electrodes set 1 cm apart in a plastic block.

Cell Counts. At each site, 12–25 sediment samples were taken for shipboard cell counts. Cells were separated from the sediment and counted using the technique of Kallmeyer et al. (21). At every site, a blank sample was processed by treating 500 μL of 0.2-μm-filtered NaCl solution like a sediment sample through the entire process of cell extraction and counting. Because absolute cell concentrations may not be accurately calculated from regression lines through log-transformed data (Fig. 2), average cell counts were calculated from nontransformed data. We used data from Parkes et al. (2) and D'Hondt et al. (19) to calculate average concentrations for previously explored communities.

Dissolved Chemical Concentrations. Interstitial waters were extracted from 5-cm-long whole rounds of cores using a Manheim-type hydraulic sediment press.

Alkalinity titrations were run on a Metrohm 809 Titrando with a Metrohm pH microelectrode, following the method of Gieskes et al. (32). Based on duplicate analyses of a control sample, precision is 0.5%.

Sulfate concentration was quantified with a Metrohm 861 Advanced Compact IC comprising an 853 CO_2 suppressor, a thermal conductivity detector, a 150- $\times$ 4.0-mm Metrosep A SUPP 5 150 column, and a 20-μL sample loop. A Metrohm 837 IC Eluent/Sample Degasser was coupled to the system. Based on duplicates, the 95% confidence limit is 0.25%.

Nitrate concentrations were analyzed with a Metrohm 844 UV/Vis Compact IC with a 150- $\times$ 4.0-mm Metrosep A SUPP 8 150 column. The pooled SD of duplicates is 0.3%.

Ex situ dissolved O_2 measurements were performed on thermally equilibrated intact whole rounds of cores. At SPG-1 and SPG-2, both custom-made microelectrodes (33) and optodes (34) were used. The optodes, connected to a Microsensor Oxygen Meter Microx TX3 (Presens GmbH), were more stable and were used for measurement at all other sites. Dissolved O_2 concentration was determined by

inserting a probe radially into the center of the core. Model calculations and radial profiles showed that the O_2 concentration in the core center of the core was not affected by ambient air on the time scales of our analyses.

For dissolved H_2 analyses, samples were collected with sterile 3-mL cutoff syringes. The sample was then extruded directly into a vial, which was immediately filled completely with distilled H_2O. A headspace was then created by injecting H_2-free gas (500 μL) through the septum while allowing an equal volume of water to escape. The H_2 was then given time to diffuse out of the interstitial water (>24 h). Three hundred microliters of the headspace gas was removed and injected into a reduced gas analyzer (Trace Analytic ta3000). The instrument was calibrated with a 100.6-ppm H_2 standard (Scott Specialty Gases). Blanks were prepared by using vials with distilled H_2O and the H_2-free headspace. The average detection limit was 67 nM H_2 (range: 2–229 nM). At SPG-1, the headspace gas was laboratory air. Because these blanks contained too much H_2 relative to the samples, we modified the procedure for the remaining sites by using bypass gas [carrier gas (N_2) that has passed over the mercury bed to remove traces of H_2] for the headspace.

Chemical calculations. Dissolved chemical fluxes were calculated using Fick's law,

$$F = (D/f) * (dC/dx),$$

where dC/dx is the gradient of the dissolved chemical concentration profile at 1.5 mbsf, D is the diffusion coefficient for the chemical in free solution, and f is the formation factor (measured as the ratio of the conductivity of seawater to the conductivity of the saturated core). Diffusion coefficients are taken from the method of Schulz (35) and corrected for a temperature of 1.5 °C [bottom water temperature in this region (36)].

Our electron transport estimates make the following assumptions. Four electrons are accepted by reducing a molecule of O_2, and 5 are accepted during reduction of NO_3^- to N_2. Eight electrons are donated by oxidizing a molecule of organic nitrogen (NH_3^+) to NO_3^-, and 2 are donated by oxidizing an H_2 molecule to H_2O. Because organic matter is a mix of molecules with carbon in different redox states, the number of electrons donated by oxidizing organic carbon is intermediate between the molecules with the most extreme redox states; because the extreme redox states of organic carbon are carbohydrates [C (0)] and lipids [C (−II)], we assume that 5 electrons are donated by oxidation of each organic carbon molecule.

H_2 yields from water radiolysis were calculated as described by Blair et al (24). These calculations use the H_2 yields of Spinks and Woods (37); decay data from Ekström and Firestone (38); and the stopping power ratios of Aitken (39) for α-, β-, and γ-radiation. Potassium-40 abundance was calculated from total potassium according to the method of Wedepohl (40). The average ^{238}U, ^{232}Th, and ^{40}K concentrations for SPG-1 to SPG-11 were assumed to be equal to the average ^{238}U, ^{232}Th, and ^{40}K concentrations for DSDP Site 595A (SPG-1) [U = 12.2 ppm (n = 9) and Th = 2.9 ppm (n = 9) (41), K = 1.56 wt% (n = 15) (42)]. The average porosity and grain density for SPG-1 to SPG-6 were assumed to be equal to the average measured porosity (82%) and grain density (2.41 g/cm^3) for SPG-1 (n = 27). The average porosity and grain density for SPG-9 to SPG-11 were assumed to be equal to the average measured porosity (76%) and grain density 2.43 g/cm^3) for SPG-9 (n = 18).

The H_2 concentrations that would be expected from radiolytic H_2 production if there were no in situ H_2 utilization were calculated from these radiolytic H_2 yields, by analytical solution of the continuity equation, using the same porosity as in the H_2 yield calculations, formation factor, and an H_2 diffusion coefficient corrected for 1.5 °C.

ACKNOWLEDGMENTS. The expedition would not have been possible without the extraordinary effort of Captain Tom Desjardins; the crew of the *RV Roger Revelle*; and Knox-02RR shipboard science party members Rika Anderson, James Dorrance, Alan Durbin, Lee Ellett, Stephanie Forschner, Ruth Fuldauer, Howard Goldstein, William Griffith, Hannah Halm, Robert Harris, Benjamin Harrison, Gregory Horn, Mark Lever, Jon Meyer, Laura Morse, Christopher Moser, Brandi Murphy, Axel Nordhausen, Lucian Parry, Ann Puschell, Justin Rogers, Bruno Soffientino, Melissa Steinman, and Paul Walczak. Coring capabilities were provided by the Oregon State University Coring Facility, directed by Nicklas Pisias and funded by the U.S. National Science Foundation (NSF) Ship Facilities Program. The cored materials and discrete samples from the expedition are curated and stored by the Marine Geological Samples Laboratory at the University of Rhode Island, directed by Steven Carey and funded by the NSF Ocean Sciences Division. This project was funded by the Ocean Drilling Program of the NSF, the National Aeronautics and Space Administration Astrobiology Institute, and the Max Planck Institute for Marine Microbiology.

1. Whelan J, et al. (1986) Evidence for sulfate-reducing and methane-producing microorganisms in sediments from Sites 618, 619, and 622. *Initial Reports Deep Sea Drilling Project 96*, eds Bouma AH, et al. (U.S. Government Printing Office, Washington), pp 767–775.
2. Parkes RJ, Cragg BA, Wellsbury P (2000) Recent studies on bacterial populations and processes in subseafloor sediments: A review. *Hydrogeology J* 8:11–28.
3. D'Hondt S, et al. (2004) Distributions of microbial activities in deep subseafloor sediments. *Science* 306:2216–2221.
4. Jørgensen BB, D'Hondt SL, Miller DJ (2006) Leg 201 synthesis: Controls on microbial communities in deeply buried sediments. *Proceedings Ocean Drilling Program, Scientific Results, 201*, eds Jørgensen BB, D'Hondt SL, Miller DJ (Ocean Drilling Program, College Station, TX), pp 1–45.
5. Jahnke RA (1996) The global ocean flux of particulate organic carbon: Areal distribution and magnitude. *Global Biogeochem Cycles* 10:71–88.
6. Schippers A, et al. (2005) Prokaryotic cells of the deep sub-seafloor biosphere identified as living bacteria. *Nature* 433:861–864.
7. Sørensen KB, Teske A (2006) Stratified communities of active archaea in deep marine subsurface sediments. *Appl Environ Microbiol* 72:4596–4603.
8. Biddle JF, et al. (2006) Heterotrophic Archaea dominate sedimentary subsurface ecosystems off Peru. *Proc Natl Acad Sci USA* 103:3846–3851.
9. Lipp JS, Morono Y, Inagaki F, Hinrichs K-U (2008) Significant contribution of Archaea to extant biomass in marine subsurface sediments. *Nature* 454:991–994.
10. Inagaki F, et al. (2006) Biogeographical distribution and diversity of microbes in methane hydrate-bearing deep marine sediments on the Pacific Ocean Margin. *Proc Natl Sci USA* 103:2815–2820.
11. Biddle JF, Fitz-Gibbon S, Schuster SC, Brenchley JE, House CH (2008) Metagenomic signatures of the Peru Margin subseafloor biosphere. *Proc Natl Acad Sci USA* 105:10583–10588.
12. Hinrichs K-U, et al. (2006) Biological formation of ethane and propane in the deep marine subsurface. *Proc Natl Acad Sci USA* 103:14684–14689.
13. D'Hondt S, Rutherford S, Spivack AJ (2002) Metabolic activity of subsurface life in deep-sea sediments. *Science* 295:2067–2070.
14. Claustre H, Maritorena S (2003) The many shades of ocean blue. *Science* 302:1514–1515.
15. Morel A, et al. (2007) Optical properties of the ''clearest'' natural waters. *Limnol Oceanogr* 52:217–229.
16. Müller RD, Roest WR, Royer J-Y, Gahagan LM, Sclater JG (1997) Digital isochrons of the world's ocean. *J Geophys Res* 102:3211–3214.
17. Rea DK, et al. (2006) Broad region of no sediment in the southwest Pacific Basin. *Geology* 34:873–876.
18. Seibold E, Berger W (1982) *The Seafloor* (Springer-Verlag, Berlin Heidelberg New York).
19. D'Hondt SL, et al. (2003) Controls on microbial communities in deeply buried sediments, Eastern Equatorial Pacific and Peru Margin, Sites 1225–1231, *Proceedings Ocean Drilling Program, Initial Reports, 201*, eds D'Hondt SL, Jørgensen BB, Miller DJ, (Ocean Drilling Program, College Station, TX).
20. Skilbeck CG, Fink, D (2006) Data report: Radiocarbon dating and sedimentation rates for Holocene-upper Pleistocene sediments, eastern equatorial pacific and Peru continental margin. *Proceedings Ocean Drilling Program, Scientific Results, 201*, eds Jørgensen BB, D'Hondt SL, Miller DJ (Ocean Drilling Program, College station, TX).
21. Kallmeyer J, Smith DC, Spivack AJ, D'Hondt S (2008) A new cell extraction procedure applied to sediments from the deep subsurface biosphere. *Limnol Oceanogr* 6:236–245.
22. Gieskes JM, Boulègue J (1986) Interstitial water studies: Leg 92, *Initial Reports Deep Sea Drilling Project 92*, eds Leinen M, Rea DK, et al. (U.S. Government Printing Office, Washington), pp 423–429.
23. Lin L-H, et al. (2005) Radiolytic H_2 in continental crust: Nuclear power for deep subsurface microbial communities. *Geochem Geophys Geosyst* 6:Q07003, 10.1029/2004GC000907.
24. Blair CC, D'Hondt S, Spivack AJ, Kingsley RH (2007) Potential of radiolytic hydrogen for microbial respiration in subseafloor sediments. *Astrobiology* 7:951–970.
25. Fischer JP, Ferdelman T, D'Hondt S, Wenzhoefer F (2007) Knox-02RR Shipboard Scientific Party Extreme oligotrophy in subsurface sediments of the South Pacific Gyre: Evidence from low oxygen fluxes. *Goechimiba et Cosmochimica Acta* 71(Suppl S):A281.
26. Price PB, Sowers T (2004) Temperature dependence of metabolic rates for microbial growth, maintenance and survival. *Proc Natl Acad Sci USA* 101:4631–4636.
27. Wang G, Spivack AJ, D'Hondt S (2006) Identification of respiration pathways in deep subseafloor sediments using a CO_2 mass-balance model. *Astrobiology* 6:230.
28. McCollom TM, Amend JP (2005) A thermodynamic assessment of energy requirements for biomass synthesis by chemolithoautotrophic micro-organisms in oxic and anoxic environments. *Geobiology* 3:135–144.
29. Verardo DJ, Froelich PN, McIntyre A (1990) Determination of organic carbon and nitrogen in marine sediments using the Carlo Erba NA-1500 Analyzer. *Deep-Sea Research* 37:157–165.
30. Zhou L, Kyte FT, Bohor BF (1991) Cretaceous/Tertiary boundary of DSDP Site 596, South Pacific. *Geology* 19:694–697.
31. Blum P (1997) *Physical Properties Handbook—A guide to the shipboard measurement of physical properties of deep-sea cores by the Ocean Drilling Program. Ocean Drilling Project Technical Note* (Ocean Drilling Program, College Station, TX).
32. Gieskes JM, Gamo T, Brumsack H (1991) *Chemical Methods for Interstitial Water Analysis aboard JOIDES Resolution, Ocean Drilling Project Technical Note 15* (Ocean Drilling Program, College Station, TX).
33. Revsbech NP, Jørgensen BB (1986) Microelectrodes: Their use in microbial ecology. *Adv Microb Ecol* 9:293–352.
34. Klimant I, Meyer V, Kühl M (1995) Fiber-optic oxygen sensors: A new tool in aquatic biology. *Limnol Oceanogr* 40:1159–1165.
35. Schulz HD (2000) Quantification of early diagenesis: Dissolved constituents in marine pore water. *Marine Geochemistry*, eds Schulz HD, Zabel M (Springer, Berlin), pp 85–128.
36. Pickard GL, Emery WJ (1982) *Descriptive Physical Oceanography: An Introduction* (Pergamon, New York), 4th Ed.
37. Spinks JWT, Woods RJ (1990) *An Introduction to Radiation Chemistry* (John Wiley & Sons, New York).
38. Ekström LP, Firestone RB (1999) World Wide Web table of radioactive isotopes, database version 2/28/99. Available at http://ie.lbl.gov/toi/index.htm. Accessed September 19, 2006.
39. Aitken MJ (1985) *Thermoluminescence Dating* (Academic, Orlando, FL).
40. Wedepohl KH (1978) *Handbook of Geochemistry* (Springer, Berlin).
41. Chan LH, Leeman WP, Plank T (2006) Lithium isotopic composition of marine sediments. *Geochem Geophys Geosyst* 7:Q06005, 10.1029/2005GC001202.
42. Plank T, Langmuir CH (1998) The chemical composition of subducting sediment: Implications for the crust and mantle. *Chem Geol* 145:325–394.